Title	Pressure-induced polar phases in multiferroic delafossite $CuFeO_2$
Author(s)	Terada Noriki, Khalyavin D. D., Manuel P., Osakabe Toyotaka, Radaelli P. G., Kitazawa Hideaki
Citation	Physical Review B, 89(22), p.220403_1-220403_6
Text Version	Publisher
URL	http://jolissrch-inter.tokai-sc.jaea.go.jp/search/servlet/search?5045628
DOI	http://dx.doi.org/10.1103/PhysRevB.89.220403
Right	©2014 The American Physical Society

PHYSICAL REVIEW B **89**, 220403(R) (2014)

Pressure-induced polar phases in multiferroic delafossite $CuFeO_2$

Noriki Terada,[1,2,3,*] Dmitry D. Khalyavin,[2] Pascal Manuel,[2] Toyotaka Osakabe,[4] Paolo G. Radaelli,[3] and Hideaki Kitazawa[1]

[1]*National Institute for Materials Science, Sengen 1-2-1, Tsukuba, Ibaraki 305-0047, Japan*

[2]*ISIS Facility, STFC Rutherford Appleton Laboratory, Chilton, Didcot, Oxfordshire OX11 0QX, United Kingdom*

[3]*Clarendon Laboratory, Department of Physics, University of Oxford, Parks Road, Oxford OX1 3PU, United Kingdom*

[4]*Japan Atomic Research Agency, Tokai, Ibaraki 319-1195, Japan*

(Received 25 February 2014; revised manuscript received 22 May 2014; published 13 June 2014)

The pressure effect on the frustrated magnetic system $CuFeO_2$ exhibiting multiferroic behavior has been studied by means of time-of-flight single crystal neutron diffraction combined with a hybrid-anvil-type pressure cell. The nonpolar collinear magnetic ground state (CM1 phase) with propagation vector $\boldsymbol{k} = (0, \frac{1}{2}, \frac{1}{2})$ turns into a proper screw magnetic ordering with incommensurate modulation $\boldsymbol{k} = (0, q, \frac{1}{2}; q \simeq 0.4)$ and a polar $21'$ magnetic point group (ICM2 phase), between 3 and 4 GPa. This spin structure is similar to the ferroelectric phase induced by magnetic field or chemical doping under ambient pressure. Above, 4 GPa, a magnetic phase (ICM3) appears, with an incommensurate propagation vector that is unique for the $CuFeO_2$ system, $\boldsymbol{k} = (q_a, q_b, q_c;\ q_a \simeq 0,\ q_b \simeq 0.34,\ q_c \simeq 0.43)$. This propagation vector at the general point results in triclinic magnetic symmetry which implies an admixture of both cycloidal and proper screw spin configurations. The ICM3 phase is stable in a narrow pressure range, and above 6 GPa, the spin-density collinear structure (ICM1 phase), similar to the first ordered state at ambient pressure, takes place. Comparing the degree of lattice distortions among the magnetic phases observed at ambient pressure, we discuss the origin of the pressure-induced magnetic phase transitions in $CuFeO_2$.

DOI: 10.1103/PhysRevB.89.220403 PACS number(s): 75.80.+q, 75.50.Ee, 77.80.−e

In the past decade, multiferroic materials where ferroelectricity coexists with (anti)ferromagnetic ordering have attracted much attention in the research field of condensed matter physics [1–3]. One of the main goals for their practical application is to control ferroelectricity/magnetism by magnetic/electric fields. Some pioneering works have demonstrated that magnetic ordering (including spin chirality) can be controlled by an electric field, and in turn, the electric polarization is tunable by an applied magnetic field [4–8]. Chemical doping also affects the magnetic and electric properties, through modified exchange interactions between spins [9–12]. As expected from several recent theoretical calculations, magnetic phase transitions inducing ferroelectricity can also be efficiently controlled by hydrostatic pressure [13,14]. However, very few experimental studies related to the pressure effect on multiferroics have been reported so far [15–18].

Although neutron diffraction is one of the most powerful techniques for magnetic structure determination, it requires relatively large samples to reliably detect magnetic reflections. This is a serious drawback for high-pressure experiments, which limits the sample size down to a small volume. Experiments on magnetic systems bring a further challenge, since low-temperature functionality of the pressure cell is required. After the introduction of the sapphire anvil pressure cells, low-temperature neutron diffraction measurements above 3 GPa have become possible [19]. Osakabe *et al.* have developed a *hybrid-anvil-type* pressure cell which combines two different anvils, WC and SiC. The cell is capable of generating pressures up to 10 GPa and can be used at low temperatures and high magnetic fields [20,21]. For more efficient use of such a well-designed pressure cell, taking advantage of the wide angle coverage detector on time-of-flight (TOF) neutron instruments is indispensable. This enables the simultaneous collection of multiple Bragg peaks. Recently, we have developed an experimental setup for high-pressure and low-temperature neutron diffraction measurements by combining the hybrid-anvil cell with the high flux TOF cold neutron diffractometer WISH [22] at the ISIS Neutron Facility [23]. In this Rapid Communication, we report the high-pressure experimental results of magnetic neutron diffraction for the multiferroic material $CuFeO_2$ by using this combination.

The delafossite compound $CuFeO_2$ is a geometrically frustrated triangular-lattice antiferromagnet which has been extensively studied to understand the subtle balance between various magnetic phases [24–27], spin-lattice coupling [28–32], and associated magnetoelectric/multiferroic phenomena [33–36]. In zero magnetic field, $CuFeO_2$ exhibits two magnetic phase transitions at $T_{N1} = 14$ K and $T_{N2} = 11$ K [24]. The magnetic ordering in the higher-temperature region, $11\ \text{K} \leqslant T \leqslant 14$ K, is a collinear spin-density wave (SDW) with incommensurate modulation, which turns into a collinear commensurate $\uparrow\uparrow\downarrow\downarrow$ structure below T_{N2} [24]. These magnetic phase transitions are accompanied by structural distortions reducing the symmetry from rhombohedral down to monoclinic and releasing the frustration [28,29]. Application of a magnetic field induces a ferroelectric phase that is stable in the $7\ \text{T} \leqslant H \leqslant 13$ T range [33]. Furthermore, the ferroelectricity in zero field can be induced by a light chemical doping, as observed in $CuFe_{1-x}B_xO_2$ (B = Al, Ga, Rh, Mn) systems [9–11,37,38]. Neutron diffraction experiments on $CuFe_{1-x}Ga_xO_2$ have revealed that the magnetic structure in the ferroelectric phase is a proper screw with an incommensurate propagation vector $\boldsymbol{k} = (0, q, \frac{1}{2}; q \simeq 0.4)$ [36]. Recently, several inelastic neutron scattering studies and theoretical calculations have suggested that the drastic change in the magnetic ground state from collinear to spiral ordering is

*TERADA.Noriki@nims.go.jp

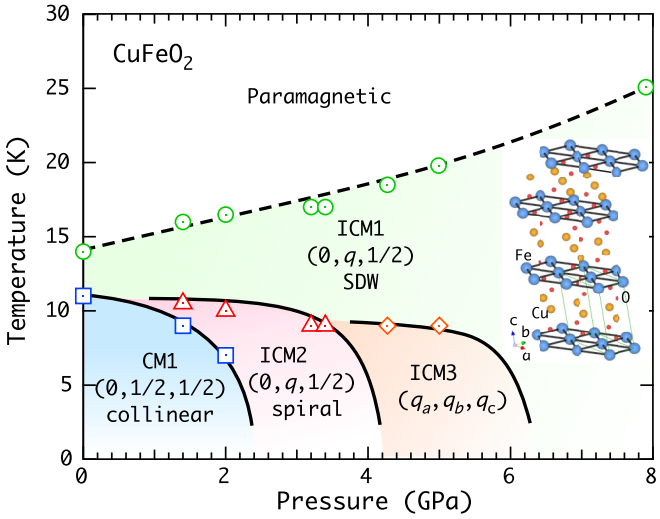

FIG. 1. (Color online) Temperature vs pressure magnetic phase diagram of $CuFeO_2$. The data at 7.9 GPa were taken from a previous paper [45]. Solid and dotted lines denote first- and second-order phase transitions, respectively.

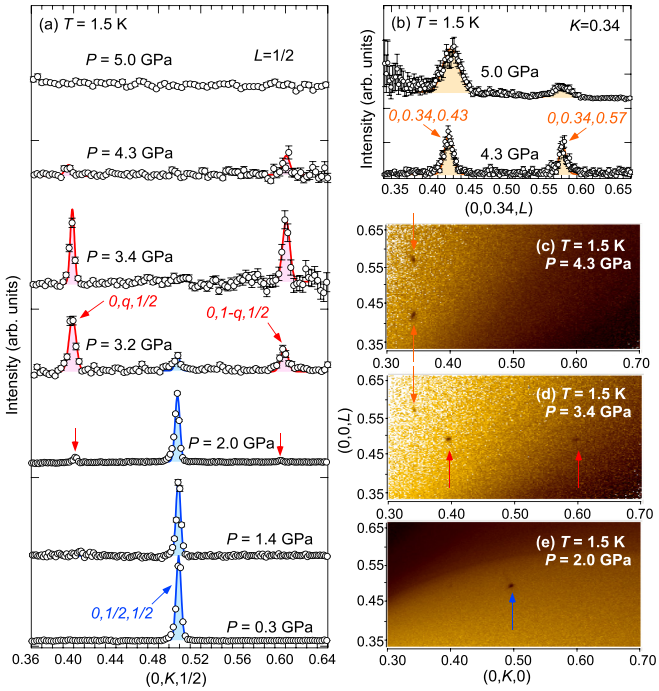

FIG. 2. (Color online) (a) Pressure dependence of the diffraction profile along the reciprocal lattice line of $(0,K,\frac{1}{2})$ at 1.5 K in $CuFeO_2$. (b) At $P = 4.3$ and 5.0 GPa, the magnetic peaks appear at the (0,0.34,0.43) and (0,0.34,0.57) positions. Neutron intensity maps on the $(0,K,L)$ plane at 1.5 K and (c) 4.3 GPa, (d) 3.4 GPa, and (e) 2.0 GPa. The arrows in (c)–(e) indicate the observed peak positions.

caused by a slight difference in exchange interactions and the anisotropy constant [39–42]. Therefore, we anticipate that the magnetic ground state in $CuFeO_2$ can also be modified by hydrostatic pressure changing the exchange and anisotropy parameters.

Xu *et al.* studied the high-pressure effect on the magnetic ordering in $CuFeO_2$ by using ^{57}Fe Mössbauer spectroscopy [43,44]. The authors observed a change in the internal fields above 6 GPa. Our previous neutron diffraction experiment at 7.9 GPa also showed that the magnetic ordering evolves from commensurate to incommensurate under pressure [45]. However, a systematic investigation to determine the magnetic structures and the detailed phase diagram still needs to be performed. In this Rapid Communication, we map out the temperature versus pressure magnetic phase diagram of $CuFeO_2$ (Fig. 1) by means of high-pressure neutron diffraction experiments. We demonstrate that hydrostatic pressure drastically changes the magnetic ground state in $CuFeO_2$, resulting in a sequence of phase transitions including a magnetic phase with an incommensurate propagation vector at a general point of the Brillouin zone.

A single crystal of $CuFeO_2$ was grown by the floating zone method [46]. The typical dimension of the sample was $0.6 \times 0.6 \times 0.2$ mm^3. A hybrid-anvil-type high-pressure cell with glycerin and a 4:1 mixture of methanol-ethanol as the pressure media for the experiments below and above 3.2 GPa, respectively [47], have been used for the neutron diffraction measurements [20,21]. The pressure was measured by the ruby fluorescence method at room temperature. The neutron diffraction data were collected on the WISH (TOF) diffractometer [22] at the ISIS Facility, U.K. The sample was mounted on a hybrid-anvil cell so that the hexagonal $[1\bar{1}0]$ axis (the monoclinic a axis) was vertical. A standard ^{4}He cryostat was used to cool the pressure cell down to 1.5 K. Magnetic structure refinements were performed using the FULLPROF program [48].

Figure 2(a) shows the pressure dependence of the diffraction profile for $CuFeO_2$ along the monoclinic $(0,K,\frac{1}{2})$ line measured at 1.5 K. Below 1.4 GPa, a magnetic peak was observed at the $(0,\frac{1}{2},\frac{1}{2})$ position [Figs. 2(a) and 2(e)] referring to the monoclinic bases defined in the inset of Fig. 1. This observation is consistent with the commensurate four-sublattice ↑↑↓↓ magnetic structure (CM1 phase) reported in a previous neutron diffraction study at ambient pressure [24]. At 2.0 GPa, a set of additional weak magnetic peaks at the positions $(0,q,\frac{1}{2}; q \simeq 0.4)$ and $(0,1-q,\frac{1}{2})$ appears, while the $0,\frac{1}{2},\frac{1}{2}$ reflection remains as the strongest component. The additional peaks belong to the ICM2 phase, which becomes dominant above 3.2 GPa [Figs. 2(a) and 2(d)]. The phase coexistence might be caused by a slight pressure inhomogeneity of the sample. The pressure-induced reflections can be assigned to the magnetic satellites $(0,0,0) + \boldsymbol{k}$ and $(0,1,1) - \boldsymbol{k}$ with the propagation vector $\boldsymbol{k} = (0,q,\frac{1}{2})$. These peak positions are almost identical to those in the ferroelectric incommensurate (FEIC) phase induced by either a magnetic field [25,29,34] or chemical doping [36]. With further increasing pressure, the peaks of the ICM2 phase decrease and almost disappear at 4.3 GPa. Instead, some other incommensurate magnetic reflections assigned to the incommensurate propagation vector $\boldsymbol{k} = (q_a,q_b,q_c;\ q_a \simeq 0,\ q_b \simeq 0.34,\ q_c \simeq 0.43)$ at the general point appear at 4.3 GPa, indicating the onset of a different ICM3 phase, as shown in Figs. 2(b) and 2(c).

The temperature dependence of the integrated intensity of the magnetic peaks at 2.0 GPa is shown in Fig. 3(a). With

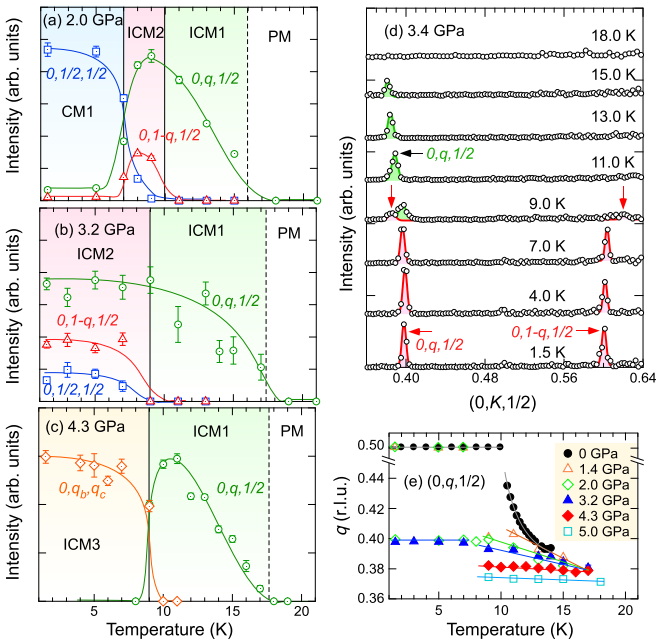

FIG. 3. (Color online) Temperature dependence of the magnetic diffraction profiles at (a) 2.0, (b) 3.2, and (c) 4.3 GPa. (d) Neutron diffraction profiles along the $(0,K,\frac{1}{2})$ reciprocal lattice line at 3.4 GPa. (e) Temperature variation of the incommensurate b component of the $(0,q,\frac{1}{2})$ propagation vector under pressure.

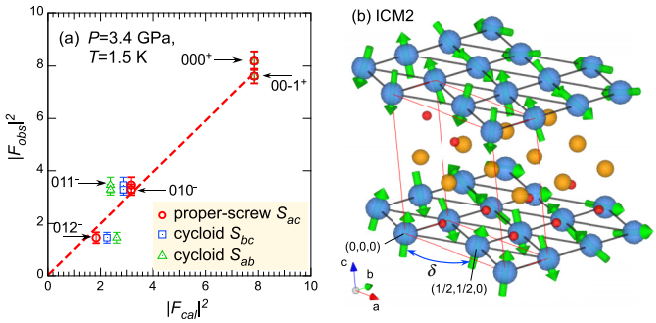

FIG. 4. (Color online) (a) Results of the magnetic structure refinements. Circles, squares, and triangles denote the structure factors calculated for the proper screw, bc-cycloid, and ab-cycloid models, respectively. The experimental data measured at 1.5 K and 3.4 GPa were corrected for absorption and the Lorentz factor. The best reliability factor, $R_F = 3.45\%$, was obtained for the model with a proper screw spin configuration in the ICM2 phase. ($R_F = 6.4\%$ for the bc-cycloid and 10.5% for the ab-cycloid model.) (b) Illustration of the proper screw magnetic structure. The image shown was depicted using the software VESTA [49].

increasing temperature, the commensurate reflection, $0,\frac{1}{2},\frac{1}{2}$, corresponding to the CM1 phase disappears at 7 K, and a set of incommensurate reflections, $0,q,\frac{1}{2}$ and $0,1-q,\frac{1}{2}$, emerges, which are characteristic of the ICM2 phase. One of the peaks in the ICM2 phase, namely, $0,1-q,\frac{1}{2}$, disappears at 10 K, revealing the phase transition from the ICM2 to ICM1 phases. This occurs because, while only a $0,q,\frac{1}{2}$ reflection is observed in the ICM1 phase, both $0,q,\frac{1}{2}$ and $0,1-q,\frac{1}{2}$ reflections appear in the ICM2 (or FEIC) phase [11,34]. The $0,q,\frac{1}{2}$ reflection survives until 16 K. Figures 3(b) and 3(d) demonstrate that the magnetic phase transition from the ICM2 to ICM1 phases occurs at 9 K and that from ICM1 to paramagnetic phases occurs at 17 K under 3.2 and 3.4 GPa. At the base temperature, we observed a couple of reflections which belong to the ICM2 phase with a small fraction of the CM1 phase, and one of the ICM2 peaks disappears at 9 K. The temperature dependence of the magnetic order parameters is almost identical to that observed in $CuFe_{1-x}Ga_xO_2$ [11]. As mentioned above, drastic changes happen in the propagation vector of $CuFeO_2$ in the ICM3 phase. As shown in Fig. 3(c), the magnetic reflections assigned to $\boldsymbol{k} = (q_a,q_b,q_c)$ with $q_a \simeq 0$, $q_b \simeq 0.34$, and $q_c \simeq 0.43$ at 4.3 GPa disappear at 9 K, and the reflections of the ICM1 phase emerge. The ICM1 phase survives down to 3 K at 7.9 GPa, which was reported in previous work [45].

It should be pointed out that the degree of temperature variation of the wave number q in the ICM1 phase is significantly suppressed by pressure, as shown in Fig. 3(e). At ambient pressure, q changes from 0.39 to 0.44 with decreasing temperature, while with increasing pressure the variation is drastically suppressed. Assuming that q is determined by an exchange parameter ratio, the temperature variation of the exchange interactions in the ICM1 phase, caused by the spin-lattice coupling, might be suppressed by pressure. To further understand the lattice distortion causing the temperature variation of the exchange interactions, high-resolution x-ray diffraction measurements under high pressure are needed.

In order to determine the magnetic structure in the ICM2 phase, we performed a magnetic structure analysis using the five magnetic reflections measured at 1.5 K and 3.4 GPa. We compared the experimental data, corrected for the Lorentz factor and absorption, with the calculated intensities in three different models: (i) a proper screw with spin components in the ac plane [see Fig. 4(b)], (ii) a cycloid with spins in the ab plane (ab cycloid), and (iii) a cycloid with b and c^* spin components (bc cycloid). The magnetic structure factor is expressed as $|F|^2 \propto f^2\mu^2[1+(\hat{\boldsymbol{Q}}\cdot\hat{\boldsymbol{n}})^2]|1\pm e^{i\delta}|^2$, where f is the magnetic form factor of Fe^{3+}, μ is the absolute value of magnetic moments, $\hat{\boldsymbol{Q}}$ and $\hat{\boldsymbol{n}}$ are unit vectors in the directions of the scattering vector and the normal vector of the spin spiral plane, respectively, and δ is the phase difference in the magnetic modulations between the (0,0,0) and $(\frac{1}{2},\frac{1}{2},0)$ sites. The plus and minus signs represent $|F|^2$ of the satellite reflections from the reciprocal lattice points where $H+K$ is the even and odd integer, respectively. As seen in Fig. 4(a), we found that the most adequate magnetic structure with the best reliability factor, $R_F = 3.45\%$, is the proper screw. The phase difference was refined to be $\delta/\pi = 0.439 \pm 0.010$, which is close to the value of the FEIC phase in the Ga-doped system ($\delta/\pi = 0.422$) [36]. The magnetic order parameter is expressed as the superposition of two identical time-odd irreducible representations of the $R\bar{3}m$ space group, $mY_1 \oplus mY_1$ combined with real and imaginary characters [50]. The proper screw ordering leaves the twofold rotation and time reversal symmetry as the point group elements, but breaks inversion and the mirror plane perpendicular to the b axis in the $C2/m$ space group of the higher-temperature ICM1 phase. The magnetic point group in the ICM2 phase is therefore the polar $21'$ that allows the ferroelectric polarization only

along the b axis. Polarization measurements under pressure for $CuFeO_2$ would be valuable to test this prediction.

On the contrary, the electric polarization in the ICM3 phase is not restricted by symmetry and takes a general direction. The general point propagation vector implies the triclinic $11'$ magnetic point group for this phase, which allows an admixture of both cycloidal and proper screw spin configurations. A quantitative refinement of such a complex structure could not be performed with the present experimental data due to the limited number of measured magnetic reflections.

Let us discuss the possible microscopic mechanisms of the symmetry-allowed electric polarization in the quantitatively characterized ICM2 phase. The inverse Dzyloshinsky-Moriya (DM) effect as formulated in Refs. [51,52] and the spin current mechanism [53], both represented by $\boldsymbol{p} \propto \boldsymbol{r}_{ij} \times (\boldsymbol{S}_i \times \boldsymbol{S}_j)(\equiv \boldsymbol{p}_1)$, are not applicable to explain the electric polarization induced by a proper screw spin ordering [54–57]. Arima has explained the ferroelectric polarization along the b axis in $CuFeO_2$ by a combined effect of d-p hybridization and spin-orbit coupling [58]. Kaplan and Mahanti have shown that an electric polarization parallel to the cross product $\boldsymbol{S}_i \times \boldsymbol{S}_j$, i.e., $\boldsymbol{p} \propto \boldsymbol{S}_i \times \boldsymbol{S}_j (\equiv \boldsymbol{p}_2)$, can actually be induced by the inverse DM effect, unless a mirror plane containing $\boldsymbol{r}_{ij}$ or a twofold rotation axis perpendicular to $\boldsymbol{r}_{ij}$ exists [59]. Proper screw magnetic ordering generates an electric polarization parallel to $\boldsymbol{S}_i \times \boldsymbol{S}_j$ in some multiferroic systems, such as $Cu_3Nb_2O_8$ [54], $CaMn_7O_{12}$ [55], and $RbFe(MoO_4)_2$ [56,57]. The electric polarization in these materials was explained by a coupling between the spin helicity $\boldsymbol{r}_{ij} \cdot (\boldsymbol{S}_i \times \boldsymbol{S}_j)$ and ferroaxial distortions $\boldsymbol{A}$ based on the inverse DM effect [54–56]. In fact, ferroaxiality of the crystal structure is the macroscopic symmetry condition necessary to ensure that the local dipoles $\propto \boldsymbol{S}_i \times \boldsymbol{S}_j$ generated by the spin canting in the consideration of Kaplan and Mahanti [59] do not macroscopically cancel each other. The case of the ICM2 phase in $CuFeO_2$ is, however, different from the cases above. The proper screw spin ordering found in the present work takes place in the nonferroaxial $R\bar{3}m$ crystal structure, but it induces ferroaxial distortions as a secondary order parameter which then couples to the helicity to generate electric polarization through the inverse DM effect.

We observed the pressure-induced phase transitions CM→ICM2→ICM3→ICM1 at low temperature. Why does pressure change the magnetic orderings in this system? Let us consider the degree of the monoclinic lattice distortion in this system. There exist some examples where lattice distortions occurring by other mechanisms, such as an electron-phonon interaction [60,61] and Jahn-Teller effect [62], are suppressed by hydrostatic pressure. One of the indices providing the degree of the monoclinic distortion is the ratio $\Delta = [b - (a/\sqrt{3})]/b_0$, where b_0 is b in the paramagnetic phase (here at 20 K) in ambient pressure. Magnetoelastic interactions couple Δ with the magnetic order parameter, providing the mechanism to control the magnetic ground state with pressure. Although we could not observe the lattice distortion under pressure in this work, we can estimate Δ in each phase at ambient pressure from previous diffraction experiments [30,35,63]. $\Delta = 0$ in the rhombohedral ($R\bar{3}m$) phase above T_{N1}, while $\Delta \neq 0$ in the monoclinic ($C2/m$ or lower) phases below T_{N1}: Δ in the CM1 phase ($T = 1.5$ K, $H = 0$ T), $\Delta_{CM1} = 4.78(1) \times 10^{-3}$ [30], $\Delta_{FEIC} = 4.10(1) \times 10^{-3}$ in the FEIC phase ($T = 1.5$ K, $H = 10$ T) [30] [$\Delta_{FEIC} = 3.95(1) \times 10^{-3}$ in zero field in a doped sample [35]], and $\Delta_{ICM1} = 0.69(2) \times 10^{-3}$ ($T = 12$ K, $H = 0$ T) in the ICM1 phase [63] under ambient pressure in $CuFeO_2$. The relationship $\Delta_{CM1} > \Delta_{FEIC} > \Delta_{ICM1}$ is consistent with the observed pressure-induced phase transitions CM1→ICM2(→ICM3)→ICM1, indicating that the pressure suppresses the structural distortions controlling the frustration in the system. We should mention here that the pressure variation of the ratio of hexagonal lattice parameters (c/a), observed at room temperature in the previous work [64], might be also one of the factors to change the magnetic ground states.

In conclusion, we have studied the pressure effect on the magnetic orderings in the strongly frustrated antiferromagnet $CuFeO_2$, by using neutron diffraction experiments under hydrostatic pressure. The main result is the pressure-temperature magnetic phase diagram (Fig. 1), consisting of the four magnetic phases including two polar ones. Below 3 GPa, the collinear CM1 phase with the commensurate propagation vector $\boldsymbol{k} = (0, \frac{1}{2}, \frac{1}{2})$ and nonpolar magnetic point group $2/m1'$ is stable at 2 K. In the 3 GPa $< P <$ 4 GPa pressure range, the ICM2 phase with the proper screw magnetic ordering and incommensurate modulation, $\boldsymbol{k} = (0, q, \frac{1}{2}; q \simeq 0.4)$, is stabilized. This polar phase with the $21'$ magnetic point group is almost identical to the FEIC phase induced by either a magnetic field [33] or chemical doping [11,36]. At 4.3 GPa, the propagation vector drastically changes from the line of symmetry to the general point, $\boldsymbol{k} = (q_a, q_b, q_c; q_a \simeq 0, q_b \simeq 0.34, q_c \simeq 0.43)$, indicating the onset of the ICM3 phase. This pressure-induced low-symmetry phase is unique for the family of delafossite multiferroics and implies an admixture of both cycloidal and proper screw spin configurations. Above ~6 GPa, the collinear ICM1 phase was found to be stable in the whole measured temperature range 3 K $\leqslant T \leqslant$ 20 K [45]. The sequence of the observed magnetic phases with changing pressure might be attributed to pressure suppression of the monoclinic lattice distortions responsible for releasing the spin frustration in the system. Additional experimental work to directly measure the lattice distortions under pressure and theoretical investigations are needed for a deeper understanding of the pressure-induced phase transitions in $CuFeO_2$.

We would like to thank John Dreyer and Matthew Tucker for their technical support for our high-pressure experiments in ISIS. This work is supported by an international collaboration research program, "Young Researcher Overseas Visits Program for Vitalizing Brain Circulation" of JSPS. N.T. is supported by the JSPS Postdoctoral Fellowships for Research Abroad.

[1] T. Kimura, T. Goto, H. Shintani, K. Ishizaka, T. Arima, and Y. Tokura, Nature (London) **426**, 55 (2003).

[2] S.-W. Cheong and M. Mostovoy, Nat. Mater. **6**, 13 (2007).

[3] Y. Tokura and S. Seki, Adv. Mater. **22**, 1554 (2010).

[4] Y. Yamasaki, H. Sagayama, T. Goto, M. Matsuura, K. Hirota, T. Arima, and Y. Tokura, Phys. Rev. Lett. **98**, 147204 (2007).
[5] T. Nakajima, S. Mitsuda, S. Kanetsuki, K. Tanaka, K. Fujii, N. Terada, M. Soda, M. Matsuura, and K. Hirota, Phys. Rev. B **77**, 052401 (2008).
[6] Y. Yamasaki, S. Miyasaka, Y. Kaneko, J.-P. He, T. Arima, and Y. Tokura, Phys. Rev. Lett. **96**, 207204 (2006).
[7] K. Kimura, H. Nakamura, S. Kimura, M. Hagiwara, and T. Kimura, Phys. Rev. Lett. **103**, 107201 (2009).
[8] Y. Kitagawa, Y. Hiraoka, T. Honda, T. Ishikura, H. Nakamura, and T. Kimura, Nat. Mater. **9**, 797 (2010).
[9] S. Kanetsuki, S. Mitsuda, T. Nakajima, D. Anazawa, H. A. Katori, and K. Prokes, J. Phys.: Condens. Matter **19**, 145244 (2007).
[10] S. Seki, Y. Yamasaki, Y. Shiomi, S. Iguchi, Y. Onose, and Y. Tokura, Phys. Rev. B **75**, 100403(R) (2007).
[11] N. Terada, T. Nakajima, S. Mitsuda, H. Kitazawa, K. Kaneko, and N. Metoki, Phys. Rev. B **78**, 014101 (2008); N. Terada, T. Nakajima, S. Mitsuda, and H. Kitazawa, J. Phys.: Conf. Ser. **145**, 012071 (2009).
[12] F. Ye, S. Chi, J. A. Fernandez-Baca, H. Cao, K.-C. Liang, Y. Wang, B. Lorenz, and C. W. Chu, Phys. Rev. B **86**, 094429 (2012).
[13] X. Rocquefelte, K. Schwarz, and P. Blaha, Sci. Rep. **2**, 759 (2012).
[14] X. Rocquefelte, K. Schwarz, P. Blaha, S. Kumarand, and J. van den Brink, Nat. Commun. **4**, 2511 (2013).
[15] H. Kimura, K. Nishihata, Y. Noda, N. Aso, K. Matsubayashi, Y. Uwatoko, and T. Fujiwara, J. Phys. Soc. Jpn. **77**, 063704 (2008).
[16] O. L. Makarova, I. Mirebeau, S. E. Kichanov, J. Rodriguez-Carvajal, and A. Forget, Phys. Rev. B **84**, 020408 (2011).
[17] D. P. Kozlenko, S. E. Kichanov, E. V. Lukin, N. T. Dang, L. S. Dubrovinsky, E. A. Bykova, K. V. Kamenev, H.-P. Liermann, W. Morgenroth, A. Ya. Shapiro, and B. N. Savenko, Phys. Rev. B **87**, 014112 (2013).
[18] T. Aoyama, A. Miyake, T. Kagayama, K. Shimizu, and T. Kimura, Phys. Rev. B **87**, 094401 (2013).
[19] I. N. Goncharenko, High Pressure Res. **24**, 193 (2004).
[20] T. Osakabe, K. Kuwahara, D. Kawana, K. Iwasa, D. Kikuchi, Y. Aoki, M. Kohgi, and H. Sato, J. Phys. Soc. Jpn. **79**, 034711 (2010).
[21] H. Yamauchi, T. Osakabe, E. Matsuoka, and H. Onodera, J. Phys. Soc. Jpn. **81**, 034715 (2012).
[22] L. C. Chapon, P. Manuel, P. G. Radaelli, C. Benson, L. Perrott, S. Ansell, N. J. Rhodes, D. Raspino, D. Duxbury, E. Spill, and J. Norris, Neutron News **22**, 22 (2011).
[23] N. Terada, T. Osakabe, D. D. Khalyavin, P. Manuel, P. G. Radaelli, and H. Kitazawa, abstract book of Joint European Magnetic Symposia (2013), p. 107 (unpublished).
[24] S. Mitsuda, N. Kasahara, T. Uno, and M. Mase, J. Phys. Soc. Jpn. **67**, 4026 (1998).
[25] S. Mitsuda, M. Mase, K. Prokes, H. Kitazawa, and H. A. Katori, J. Phys. Soc. Jpn. **69**, 3513 (2000).
[26] O. A. Petrenko, G. Balakrishnan, M. R. Lees, D. M. Paul, and A. Hoser, Phys. Rev. B **62**, 8983 (2000).
[27] T. T. A. Lummen, C. Strohm, H. Rakoto, and P. H. M. van Loosdrecht, Phys. Rev. B **81**, 224420 (2010).
[28] N. Terada, S. Mitsuda, H. Ohsumi, and K. Tajima, J. Phys. Soc. Jpn. **75**, 023602 (2006).
[29] F. Ye, Y. Ren, Q. Huang, J. A. Fernandez-Baca, P. Dai, J. W. Lynn, and T. Kimura, Phys. Rev. B **73**, 220404(R) (2006).
[30] N. Terada, Y. Tanaka, Y. Tabata, K. Katsumata, A. Kikkawa, and S. Mitsuda, J. Phys. Soc. Jpn. **75**, 113702 (2006); **76**, 068001 (2007).
[31] N. Terada, Y. Narumi, Y. Sawai, K. Katsumata, U. Staub, Y. Tanaka, A. Kikkawa, T. Fukui, K. Kindo, T. Yamamoto, R. Kanmuri, M. Hagiwara, H. Toyokawa, T. Ishikawa, and H. Kitamura, Phys. Rev. B **75**, 224411 (2007).
[32] G. Quirion, M. L. Plumer, O. A. Petrenko, G. Balakrishnan, and C. Proust, Phys. Rev. B **80**, 064420 (2009).
[33] T. Kimura, J. C. Lashley, and A. P. Ramirez, Phys. Rev. B **73**, 220401(R) (2006).
[34] N. Terada, S. Mitsuda, Y. Tanaka, Y. Tabata, K. Katsumata, and A. Kikkawa, J. Phys. Soc. Jpn. **77**, 054701 (2008).
[35] T. Nakajima, S. Mitsuda, T. Inami, N. Terada, H. Ohsumi, K. Prokes, and A. Podlesnyak, Phys. Rev. B **78**, 024106 (2008).
[36] T. Nakajima, S. Mitsuda, K. Takahashi, M. Yamano, K. Masuda, H. Yamazaki, K. Prokes, K. Kiefer, S. Gerischer, N. Terada, H. Kitazawa, M. Matsuda, K. Kakurai, H. Kimura, Y. Noda, M. Soda, M. Matsuura, and K. Hirota, Phys. Rev. B **79**, 214423 (2009).
[37] E. Pachould, C. Martina, B. Kundys, C. Simon, and A. Maignan, J. Solid State Chem. **183**, 344 (2010).
[38] K. Hayashi, R. Fukatsu, T. Nozaki, Y. Miyazaki, and T. Kajitani, Phys. Rev. B **87**, 064418 (2013).
[39] F. Ye, J. A. Fernandez-Baca, R. S. Fishman, Y. Ren, H. J. Kang, Y. Qiu, and T. Kimura, Phys. Rev. Lett. **99**, 157201 (2007).
[40] T. Nakajima, A. Suno, S. Mitsuda, N. Terada, S. Kimura, K. Kaneko, and H. Yamauchi, Phys. Rev. B **84**, 184401 (2011).
[41] J. T. Haraldsen, F. Ye, R. S. Fishman, J. A. Fernandez-Baca, Y. Yamaguchi, K. Kimura, and T. Kimura, Phys. Rev. B **82**, 020404 (2010).
[42] T. Nakajima, N. Terada, S. Mitsuda, and R. Bewley, Phys. Rev. B **88**, 134414 (2013).
[43] W. M. Xu, M. P. Pasternak, and R. D. Taylor, Phys. Rev. B **69**, 052401 (2004).
[44] W. M. Xu, G. Kh. Rozenberg, M. P. Pasternak, M. Kertzer, A. Kurnosov, L. S. Dubrovinsky, S. Pascarelli, M. Munoz, M. Vaccari, M. Hanfland, and R. Jeanloz, Phys. Rev. B **81**, 104110 (2010).
[45] N. Terada, T. Osakabe, and H. Kitazawa, Phys. Rev. B **83**, 020403 (2011).
[46] T. R. Zhao, M. Hasegawa, and H. Takei, J. Cryst. Growth **166**, 408 (1996).
[47] T. Osakabe and K. Kakurai, Jpn. J. Appl. Phys. **47**, 6544 (2008).
[48] J. Rodriguez-Carvajal, Physica B **192**, 55 (1993).
[49] K. Momma and F. Izumi, J. Appl. Crystallogr. **41**, 653 (2008).
[50] B. J. Campbell, H. T. Stokes, D. E. Tanner, and D. M. Hatch, J. Appl. Crystallogr. **39**, 607 (2006).
[51] M. Mostovoy, Phys. Rev. Lett. **96**, 067601 (2006).
[52] I. A. Sergienko and E. Dagotto, Phys. Rev. B **73**, 094434 (2006).
[53] H. Katsura, N. Nagaosa, and A. V. Balatsky, Phys. Rev. Lett. **95**, 057205 (2005).
[54] R. D. Johnson, Sunil Nair, L. C. Chapon, A. Bombardi, C. Vecchini, D. Prabhakaran, A. T. Boothroyd, and P. G. Radaelli, Phys. Rev. Lett. **107**, 137205 (2011).

[55] R. D. Johnson, L. C. Chapon, D. D. Khalyavin, P. Manuel, P. G. Radaelli, and C. Martin, Phys. Rev. Lett. **108**, 067201 (2012).
[56] A. J. Hearmon, F. Fabrizi, L. C. Chapon, R. D. Johnson, D. Prabhakaran, S. V. Streltsov, P. J. Brown, and P. G. Radaelli, Phys. Rev. Lett. **108**, 237201 (2012).
[57] M. Kenzelmann, G. Lawes, A. B. Harris, G. Gasparovic, C. Broholm, A. P. Ramirez, G. A. Jorge, M. Jaime, S. Park, Q. Huang, A. Ya. Shapiro, and L. A. Demianets, Phys. Rev. Lett. **98**, 267205 (2007).
[58] T. Arima, J. Phys. Soc. Jpn. **76**, 073702 (2007).
[59] T. A. Kaplan and S. D. Mahanti, Phys. Rev. B **83**, 174432 (2011).
[60] T. Ishidate, S. Abe, H. Takahashi, and N. Mori, Phys. Rev. Lett. **78**, 2397 (1997).
[61] J. P. Itié, B. Couzinet, A. Polian, A. M. Flank, and P. Lagarde, Eur. Phys. Lett. **74**, 706 (2006).
[62] F. Aguado, F. Rodríguez, R. Valiente, J. P. Itié, and P. Munsch, Phys. Rev. B **70**, 214104 (2004).
[63] N. Terada *et al.* (unpublished).
[64] T. R. Zhao, M. Hasegawa, T. Kondo, T. Yagi, and H. Takei, Mater. Res. Bull. **32**, 151 (1997).